Biochimica et Biophysica Acta 1808 (2011) 405–414

Contents lists available at ScienceDirect

Biochimica et Biophysica Acta

journal homepage: www.elsevier.com/locate/bbamem

Ethanol effects on binary and ternary supported lipid bilayers with gel/fluid domains and lipid rafts

Joaquim T. Marquês, Ana S. Viana, Rodrigo F.M. De Almeida *

Centro de Química e Bioquímica, Faculdade de Ciências da Universidade de Lisboa, Ed. C8, Campo Grande 1749-016, Lisboa, Portugal

ARTICLE INFO

Article history:
Received 14 July 2010
Received in revised form 8 October 2010
Accepted 12 October 2010
Available online 15 October 2010

Keywords:
Ethanol–membrane interactions
Liquid AFM
Liquid ordered liquid disordered
Bilayer expansion
Silicon
Sphingomyelin

ABSTRACT

Ethanol–lipid bilayer interactions have been a recurrent theme in membrane biophysics, due to their contribution to the understanding of membrane structure and dynamics. The main purpose of this study was to assess the interplay between membrane lateral heterogeneity and ethanol effects. This was achieved by *in situ* atomic force microscopy, following the changes induced by sequential ethanol additions on supported lipid bilayers formed in the absence of alcohol. Binary phospholipid mixtures with a single gel phase, dipalmitoylphosphatidylcholine (DPPC)/cholesterol, gel/fluid phase coexistence DPPC/dioleoylphosphatidylcholine (DOPC), and ternary lipid mixtures containing cholesterol, mimicking lipid rafts (DOPC/DPPC/cholesterol and DOPC/sphingomyelin/cholesterol), i.e., with liquid ordered/liquid disordered (ld/lo) phase separation, were investigated. For all compositions studied, and in two different solid supports, mica and silicon, domain formation or rearrangement accompanied by lipid bilayer thinning and expansion was observed. In the case of gel/fluid coexistence, low ethanol concentrations lead to a marked thinning of the fluid but not of the gel domains. In the case of ld/lo all the bilayer thins simultaneously by a similar extent. In both cases, only the more disordered phase expanded significantly, indicating that ethanol increases the proportion of disordered domains. Water/bilayer interfacial tension variation and freezing point depression, inducing acyl chain disordering (including opening and looping), tilting, and interdigitation, are probably the main cause for the observed changes. The results presented herein demonstrate that ethanol influences the bilayer properties according to membrane lateral organization.

1. Introduction

In the last decades, the importance of the lipid components of the bilayer, especially their lateral organization into microdomains with different physical properties, was established [1,2]. Currently, it is widely accepted that the plasma membrane of many cell types is highly compartmentalized and organized into domains in different time and length scales, with differentiated lipid–lipid interactions [3]. The most widely investigated domains are the sphingolipid/cholesterol-enriched domains known as lipid rafts [4–7]. It was also established from biophysical studies that to model the properties of these domains it is necessary to use a ternary lipid mixture of cholesterol and two other lipids (phospho or sphingolipids) differing significantly in their main transition temperature (T_m) [8–10]. More recently, the formation of high T_m sphingolipid-enriched domains with properties similar to the lipid gel phase that is commonly found in model systems has been gaining strength [11]. It is thus important in studies of membrane related phenomena to account for the dynamic role of membrane lipid composition and organization into nano or microdomains.

One significant area of study with lipid bilayers has been their interaction with ethanol. Understanding ethanol–lipid interactions has helped to unravel membrane biophysical properties and elucidate the mechanism of action of other small molecules with anaesthetic properties [12–14]. This subject is also relevant for human health, e.g. [15–17], and for a significant number of experiments which require the addition of external components, such as probes or drugs, in ethanol solutions to liposomes or cells [18]. Moreover, it is necessary to the understanding of the adaptation of organisms performing alcoholic fermentation to high ethanol levels in the growing medium [19].

Most biophysical studies of ethanol–bilayer interactions have been conducted using bulk techniques, such as X-ray scattering [20,21], differential scanning calorimetry (DSC) [21–23], fluorescence spectroscopy [22,24–26], NMR [27,28], and EPR [29]. Importantly, it was determined that ethanol binds to the lipid–water interface [28] and promotes the disordering of the acyl chains [27]. Furthermore, the induction of bilayer thickness reduction has been reported, which may occur mainly by three processes—disordering [21,30,31], tilt angle change [21,32] or interdigitation of phospholipid acyl chains [20,21]. This last mechanism is characterized by the interpenetration of the acyl chains from one bilayer leaflet into the other with the consequent bilayer

* Corresponding author. Tel.: +351 217500924; fax: +351 217500088.
E-mail address: rodrigo.almeida@fc.ul.pt (R.F.M. De Almeida).

0005-2736/$ – see front matter © 2010 Elsevier B.V. All rights reserved.
doi:10.1016/j.bbamem.2010.10.006

thinning. The increase of the mean molecular area results in a lateral expansion of the bilayer [20,33]. In addition, phospholipid/ethanol phase diagrams were established, which show that below the phospholipid T_m, i.e., in the gel phase, it is possible to have coexistence of an interdigitated and a non-interdigitated phase [21]. The ethanol/DPPC phase diagrams indicate that the threshold for interdigitated domain formation should be between 3.2% [21] and 5% [33] ethanol, and that the bilayer should be fully interdigitated for 10–12% of this alcohol. However, more recently, it was shown by atomic force microscopy (AFM) that overnight incubation of a fluid phospholipid bilayer with ethanol also promoted the formation of height-reduced domains coexisting with unchanged portions of the bilayer [12]. The use of AFM also helped to elucidate the events by which some anaesthetics, such as halothane and ethanol, or antibiotics exert their actions [12,34].

Detailed studies of the effect of ethanol on lipid mixtures are scarce despite the evidence suggesting that the outcome should be highly dependent on the phase behaviour of the system [35–37]. It was found by DSC and fluorescence spectroscopy that cholesterol in small concentration (2 mol%) enhances ethanol effects [22], whereas in high concentrations (20 mol%) cholesterol has a protective action, preventing interdigitation [24]. These studies were conducted in binary mixtures with no lipid phase separation. Recently, an AFM study reported a similar effect for DPPC/ergosterol bilayers [38]. To the best of our knowledge, a study of ethanol interaction with lipid raft-forming bilayers, i.e., ternary lipid mixtures with liquid ordered (lo)/liquid disordered (ld) phase separation, was not yet performed, whereby the role of lipid domains on ethanol-induced effects remains undisclosed. Considering the vital functions associated with lipid rafts, such as protein sorting, signal transduction and internalization of pathogens [39–41], it is significant to establish the interactions between ethanol and raft-forming bilayers.

In the present work, the interactions of ethanol with distinct lipid bilayers containing no domains, gel/fluid domains, and lipid rafts models were studied. *In situ* tapping-mode AFM using a liquid cell was performed in order to follow in real time the dynamic morphological changes of the supported lipid bilayer (SLB) induced by increasing ethanol concentrations. SLBs were prepared on two different substrates, mica and silicon. Mica is a well-known substrate for successful lipid deposition and AFM imaging [42–44] and silicon is much less explored, despite its unique optical properties [45,46]. In addition, many of the technologies currently used and in development are silicon based, and the improvement of the deposition of lipid bilayers in silicon and their characterization offer potentially new applications for SLB (e.g. [47–49]). Additionally, the use of two distinct solid supports stems from the possibility that membrane–substrate interactions may affect the formation and dynamics of lipid domains [44]. Regarding the effect of ethanol on silicon SLBs, Miszta et al. [50] did not detect ethanol-induced thinning in fluid bilayers composed of DOPC, DLPC and DOPC/DOPS using conventional ellipsometry. However, Gedig et al. [51] used imaging ellipsometry and they were able to observe ethanol-induced thickness reduction in gel and fluid phase dimiristoylphosphatidylcholine (DMPC) bilayers deposited on silicon.

The results here presented show the lateral reorganization of the lipid bilayer from the nano to the microscale, and the alterations in the height of the domains at a sub-nanometer scale. The changes observed are highly dependent on the previous organization and nature of the lipid domains or rafts. The contributions of water/bilayer interfacial tension reduction, freezing point depression, disordering/tilting of acyl chains and interdigitation in relation to the domain (re) organization of the bilayer are discussed.

2. Materials and methods

2.1. Chemicals

1,2-Dipalmitoyl-*sn*-glycero-3-phosphocholine (DPPC), 1,2-dioleoyl-*sn*-Glycero-3-phosphocholine (DOPC) and *N*-palmitoyl-D-*erythro*-sphingosylphosphorylcholine or *N*-palmitoyl-sphingomyelin (PSM) were purchased from Avanti Polar Lipids (Alabaster, AL); cholesterol was purchased from Sigma (St. Louis, MO). Other reagents were of the highest purity available.

Three buffers were used for hydration of lipid mixtures and AFM imaging: buffer A—10 mM Hepes, 150 mM NaCl, pH 7.4; buffer B—10 mM Hepes, 150 mM NaCl, 3 mM $CaCl_2$, pH 7.4; buffer C—2.71 mM K_2HPO_4, 1.54 mM NaH_2PO_4, 154 mM NaCl, pH 7.4.

2.2. Phospholipid and cholesterol quantification

The phospholipid concentration was determined gravimetrically and by inorganic phosphate quantification [52]. Cholesterol quantification was made by gravimetry.

2.3. Preparation of supported lipid bilayers on mica and silicon

Lipid stock solutions and lipid mixtures were prepared with spectroscopic grade chloroform from Merck (Darmstadt, Germany). The solvent was evaporated first under a mild flow of nitrogen, followed by overnight vacuum. The lipids were hydrated with buffer A, for mica, or C for silicon, which were shown to be the most appropriate buffers to form SLBs on those substrates ([53] and [45], respectively). To confirm this literature result, other buffers were essayed, including using buffer A for silicon and buffer C for mica, and the quality of the SLBs obtained was inferior (data not shown). The lipid was suspended by vortex stirring and freeze-thaw cycles (total lipid concentration 10 mg/mL). Small unilamellar vesicles (SUV) were made by power sonication (Hielscher, UP200S). For deposition on mica, 10 μL of SUV suspension was diluted in 140 μL buffer B [54] and deposited on freshly cleaved mica (Veeco) and incubated for 30 min at 70 °C. After this incubation step the samples were left at room temperature to cool for 1 h and SLB were washed several times with buffer A at room temperature (20 °C).

Silicon oxide wafers (provided by Institute of Mechanics, Beijing, PRC) were washed in a freshly prepared piraña solution (sulfuric acid and hydrogen peroxide 3:1) for ca. 5 min and maintained in water until use. Before lipid deposition the silicon wafers were dried under a nitrogen flow. Large unilamellar vesicles (LUV) were prepared by extrusion in an Avanti Mini-extruder at 60 °C using polycarbonate filters with 100 nm pore diameter (Whatman). LUV suspension (100 μL) was added to the silicon oxide wafer and incubated for 30 min at 60 °C. Again, after this incubation step the samples were left at room temperature to cool for 1 h and SLB was washed by immersion in buffer C at 20 °C.

2.4. AFM imaging

The procedure was identical for both mica and silicon substrates. AFM *in situ* measurements, i.e., with the sample immersed in buffer recurring to a liquid cell, were performed at room temperature using a Multimode Nanoscope IIIa Microscope (Digital Instruments, Veeco). Topographic images were taken with a scan rate of ca. 2 Hz in tapping mode, where the use of an oscillating probe drastically reduces the force applied to the sample during the scanning [42], as compared to the measurements performed in contact mode [55], since the cantilever only touches the surface after one oscillation cycle. A sequence of different scanned areas containing the same bilayer region was included in Supplementary Fig. S1, in order to demonstrate that tip scanning had no effect on the height, shape and domain organization of the lipid bilayer.

Before each experiment, the glass block holding the cantilever was washed several times with water and ethanol. The cantilevers used were made of silicon nitride (NPS, ca. 0.58 N/m of spring constant, Veeco) with a resonance frequency in liquid of about 9 kHz. The samples were initially covered with 45 μL of buffer A for mica SLBs or buffer C for silicon SLBs.

When a stable image in a region of interest of the SLB in a buffered solution was obtained, successive additions of ethanol were performed and the same region was imaged between each addition. In many cases, regions where the coverage by lipid was incomplete, and where the lipid bilayer has a distinctive shape were chosen on purpose, in order to easily identify the changes in lateral organization of the membrane upon successive additions of ethanol. To fully appreciate bilayer expansion, it was necessary to have images where the area coverage was around 50% before ethanol addition. The images presented in this study are representative of each sample (the observations are uniform for the whole sample); at least 3 independent experiments on freshly prepared SLB have been performed for each lipid system. To obtain the thickness values (or thickness differences) for each sample, at least 10 different profiles were drawn, and the median value taken. The values of thickness in Table 1 are the average ± standard deviation of the values from all the experiments, and the most representative profiles were selected for the figures shown. The estimation of the area corresponding to the different types of domains was performed using the software ImageJ. All the domains of a specific thickness were added to obtain the total phase area.

3. Results

3.1. Interaction of ethanol with lipid bilayers displaying gel/fluid phase coexistence

At room temperature, the binary lipid system DOPC/DPPC displays a range of compositions for which a gel phase rich in DPPC coexists with a fluid phase rich in DOPC [56,57]. Accordingly, DOPC/DPPC (1:1 mol:mol) bilayers deposited on mica were used to address the influence of gel/fluid domains on ethanol-induced membrane changes. In Fig. 1, panel a, the phase coexistence is clearly observed by AFM, since the lipid bilayer is heterogeneous, presenting domains with distinct thickness. The height of thicker (6.4 nm) and thinner (5.2 nm) domains in coexistence is very similar to the respective thickness of the phases formed by the two pure lipids DPPC (6.4 nm) and DOPC (5.3 nm) as shown in the topographical profiles of Supplementary Fig. S2a and b, respectively. Since the T_m of DPPC is 41 °C, the lipid bilayer is in the gel phase [58]. The T_m of DOPC is −22 °C [59]; thus at room temperature, the lipid bilayer formed is clearly in the fluid phase [56]. This allows unambiguous assignment of the thicker and thinner domains observed in the binary mixture to the gel and to the fluid, respectively. The thickness gap between coexisting domains in DOPC/DPPC is thus 1.2 nm, as also found by other authors [34,60]. The thickness of the bilayers with or without phase coexistence, and height differences, are summarized in Table 1. The area fraction of gel/fluid phases was also calculated (Table 2), and is in agreement with the molar fractions predicted by the DOPC/DPPC (24% gel, 76% fluid) phase diagram according to the lever rule, after correction for the different mean molecular area of each phase [56].

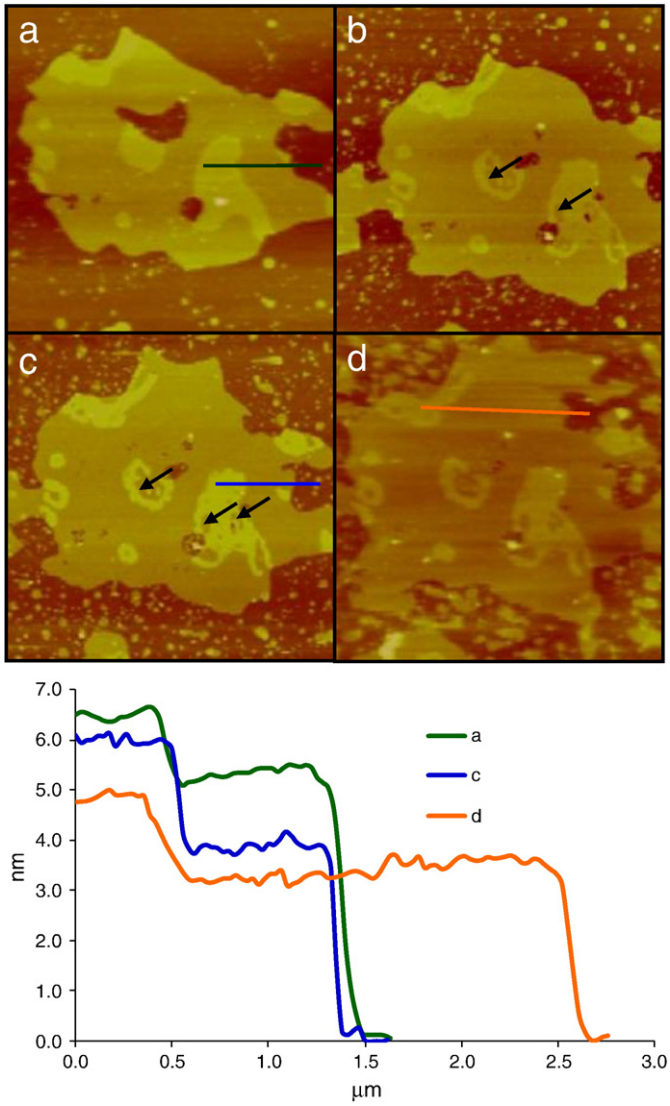

Fig. 1. Ethanol interactions with a bilayer with gel/fluid phase coexistence. AFM image of an SLB composed of DOPC/DPPC (1:1) deposited on mica, (a) in the absence of ethanol, and after successive additions of ethanol to a final concentration of (b) 11%, (c) 22%, and (d) 34% (v/v) in Hepes buffer. The images were obtained in a liquid cell at room temperature. The inset shows the topographical profiles corresponding to the colored lines in panels a–d. The images correspond to an area of 5 µm × 5 µm. $Z = 24$ nm. The black arrows indicate fluid domains that form inside gel domains.

Table 1
Bilayer thickness values for different lipid systems deposited on mica and silicon before and after final ethanol (EtOH) addition. When different types of domains coexist, their height differences are also indicated. The data presented correspond to the average ± standard deviation, obtained as described under Materials and Methods. Chol stands for cholesterol.

	Lipid system	Bilayer thickness	Domain height difference	Height reduction after EtOH addition
Mica	DPPC/Chol (98:2)	6.4 ± 0.3		1.9 ± 0.2
	DOPC/DPPC (1:1)[a]	6.4 ± 0.3 (g)	1.2 ± 0.2	0.4 + 1.1 = 1.5 ± 0.2 (g)[b]
		5.2 ± 0.2 (f)		1.3 + 0.3 = 1.6 ± 0.2 (f)[b]
	DOPC/DPPC/Chol (40:40:20)[c]	6.5 ± 0.3 (lo)	1.2 ± 0.2	1.1 ± 0.2
		5.3 ± 0.2 (ld)		
	DOPC/PSM/Chol (40:40:20)[c]	6.0 ± 0.3 (lo)	1.0 ± 0.2	1.0 ± 0.2
		5.0 ± 0.2 (ld)		1.2 ± 0.2
Silicon	DPPC	6.2 ± 0.3		1.8 ± 0.2
	DOPC/PSM/Chol (40:40:20)[c]	6.6 ± 0.3 (lo)	1.1 ± 0.2	1.3 ± 0.2
		5.5 ± 0.2 (ld)		

[a] Gel (g)/fluid (f) phases.
[b] First thickness reduction + second thickness reduction.
[c] Liquid ordered (lo)/liquid disordered phases (ld) (lipid rafts).

Sequential additions of ethanol to the mixed DOPC/DPPC SLB on mica were performed in the liquid cell. When 11% (v/v) ethanol is reached the only detectable change is the appearance of fluid patches within the former gel domains, whereas in the presence of 22% (v/v) of ethanol (Fig. 1b and c), the thickness of both fluid and gel domains decreased, as illustrated in the topographical profile of panel c (the corresponding profile for panel b (not shown) is identical to the one for panel a). However, the height of the gel decreased only by ~0.4 nm, whereas that of the fluid decreased by 1.3 nm. Under such conditions, the height difference between gel and fluid phases is maximal, with a value of ~2.1 nm. The lower height effect on the gel has been observed for all the scanned regions and is in agreement

Table 2
Estimation of bilayer area and volume for lipid phases of SLBs deposited on mica, unless otherwise stated. Initial area (A_i) and volume (V) refers to the values before ethanol addition. Final area values were experimentally obtained ($A_{f\ Exp}$) or calculated considering volume conservation ($A_{f\ Calc}$). f, fluid; g, gel; ld, liquid disordered; lo, liquid ordered. All the calculations were performed based on 400 μm^2 AFM images except for DOPC/DPPC and DOPC/PSM/cholesterol deposited on silicon for which the calculations were based on 64 μm^2 and 9 μm^2 images, respectively. Chol stands for cholesterol.

Lipid system			A_i (nm^2)×10^7	Area fraction	V (nm^3)×10^7	A_f (nm^2)×10^7		$A_{f\ Exp}/A_i$
						Calc.	Exp.	
DOPC/DPPC		f	1.3	0.80	6.8	1.8	2.0 (34% EtOH)	1.5
		g	0.3	0.20	2.1	0.4	0.3 (34% EtOH)	0.9
DOPC/DPPC/Chol		ld	10.0	0.68	54.0	11.2	15.2 (13% EtOH)	1.5
							34.9 (25% EtOH)	3.5
		lo	4.5	0.32	30.0	5.5	5.2 (13% EtOH)	1.2
							4.6 (25% EtOH	1.0
DOPC/PSM/Chol		ld	13.7	0.57	73.7	15.5	22.4 (13% EtOH)	1.7
		lo	10.7	0.43	69.5	11.8	11.5 (13% EtOH)	1.1
	Silicon	ld	0.5	0.92	2.7	0.6	0.6 (13% EtOH)	1.3
		lo	0.04	0.08	0.3	0.05	0.03 (13% EtOH)	0.9

with a previous observation by Vierl et al. [21]. In that study, X-ray diffraction was used to investigate ethanol-induced interdigitation in DPPC liposome suspension. The authors observed a 0.2 nm reduction of the lamellar repeat distance, which was attributed to an alteration of the tilt angle of the acyl chains in relation to the bilayer normal.

In addition, the fraction of fluid domains in relation to gel ones increased, because fluid domains appear within regions that in the absence of ethanol (panel a) were occupied by gel phase (arrows in panels b and c; Table 2; see also Supplementary Fig. S3). Finally, with 34% (v/v) of ethanol, the gel becomes much thinner, and the fluid phase also presents a more extensive thickness reduction, originating a gel/fluid height gap of ~1.3 nm which is similar to the one in the absence of ethanol. A marked expansion of the fluid phase can be also observed (see Table 2 for quantification), while gel domains maintain their identity.

The fact that the fluid undergoes a more significant thickness reduction before the gel is in agreement with the need for a lower ethanol concentration to induce the formation of thinned domains in pure DOPC than in pure DPPC, as reported in the literature. In a previous study, it was shown that domains of reduced thickness appeared in DOPC bilayers for concentrations of alcohol that had no effect on DPPC [12].

An interesting observation is that the site of formation of thinned domains depends on lipids proportion and domain arrangement. In Fig. 1 described above, the bilayer is composed of gel domains in a continuous fluid, and the thinned fluid domains form within the gel domains. In Fig. 2, an image of the DOPC/DPPC mixture is shown, in this case with a molar ratio of 8:92. In opposition to the mixture shown in Fig. 1, the majority of the bilayer is now in the gel phase, which is the continuous phase, surrounding fluid phase domains. The thickness reduction of fluid domains is observed first in the interface between gel and fluid regions of the bilayer. The formation of those domains gives rise to "islands" of unmodified fluid, and generates topographical profiles as the one shown in Fig. 2.

The observations described above seem to be in contradiction with the hydrophobic matching principle, since an increased height difference at the domain interface implies a higher exposure of the hydrophobic portion of the gel phase lipids to the water phase [61]. However, such behavior could be explained by an accumulation of ethanol molecules in interfacial regions, thereby protecting the acyl chains of gel phase lipids from exposure to water.

3.2. Ethanol-induced membrane effects in a binary single-phase bilayer

It was previously shown, through a fluorescence spectroscopy method used in liposome suspensions, that cholesterol at low concentrations can have a facilitating effect regarding ethanol interaction in the system DPPC/cholesterol (98:2 mol:mol) [22]. In the present study, SLBs with the same composition were prepared on mica, and the effect of ethanol followed by AFM. A result concurrent with the literature was obtained, as described in Fig. 3. It is shown that i) in the absence of ethanol the thickness of the bilayer is similar to that of pure DPPC (see Supplementary Fig. S2); ii) 11% (v/v) of ethanol induces the thickness reduction by approximately 2 nm of a substantial fraction of the bilayer and its expansion. The effect was much more pronounced than the ones observed for DOPC-enriched fluid and even more so for DPPC-enriched gel in the DOPC/DPPC mixtures described above. Thus, the facilitating effect previously reported [22] is also observed for SLBs of the same composition. This promotion probably stems from the perturbation that a small amount of cholesterol induces in the gel phase, which becomes less compact or more defective allowing for a better penetration of small molecules such as ethanol. Interestingly, ergosterol apparently does not have this enhancing effect at low concentrations [38].

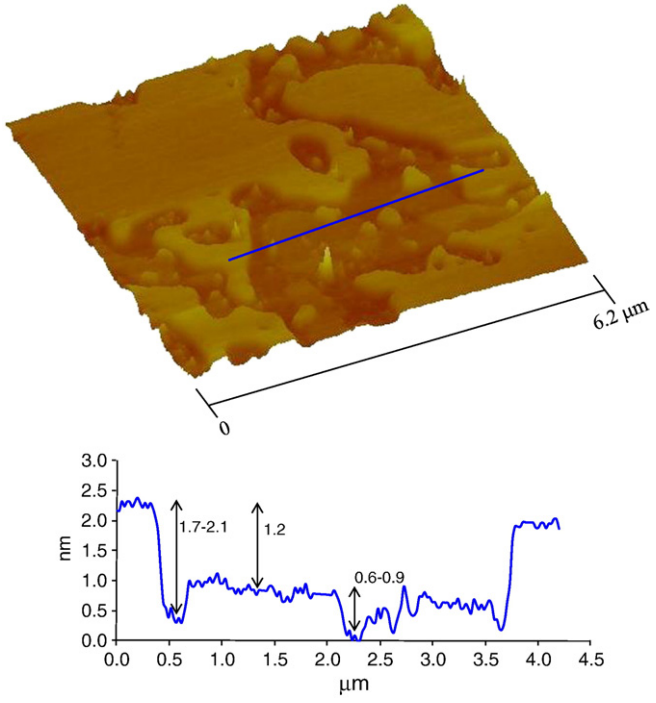

Fig. 2. The topology of gel/fluid domains modulates ethanol interactions with the lipid bilayer. AFM image of an SLB composed of DOPC/DPPC (8:92 mol:mol) deposited on mica, after successive additions of ethanol to a final concentration of 18% (v/v) in Hepes buffer. The image was obtained in a liquid cell at room temperature. The inset shows the topographical profile corresponding to the colored line in the main panel. $Z = 10$ nm. The numbers indicated next to the arrows correspond to a height difference.

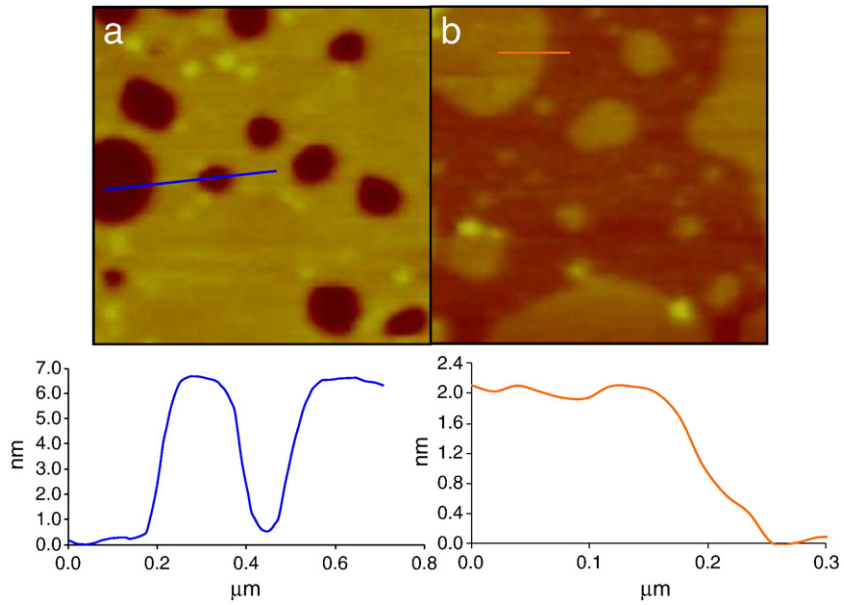

Fig. 3. Effect of cholesterol in small amounts on the alterations induced by ethanol in a gel phase bilayer. Top row: AFM images of DPPC/cholesterol 98:2 SLB on mica with 1.4 μm × 1.4 μm obtained in Hepes buffer at room temperature: (a) in the absence of ethanol, and (b) after addition of ethanol 11% (v/v). $Z = 15$ nm (a); $Z = 20$ nm (b). Bottom row: topographical profiles corresponding to the colored lines in the top row images. From the blue line it is possible to determine the original bilayer thickness; from the orange line it is possible to determine the height difference between interdigitated and non-interdigitated domains. The bright round features correspond to incompletely fused vesicles, and not to lipid domains.

3.3. Interaction of ethanol with raft-forming ternary lipid mixtures

Ternary lipid mixtures displaying lo/ld phase separation are good models of the lipid domains known as lipid rafts that occur in many cellular membranes as described in the Introduction section. In the present study, two ternary mixtures were used: DOPC/DPPC/cholesterol and DOPC/PSM/cholesterol both with molar ratios of 40:40:20. According to the ternary phase diagrams reported for these mixtures [56,62], for that molar ratio, the systems lay in the lo/ld coexistence region, with ca. 40% mol fraction of lo phase. The lo phase corresponds to the high T_m lipid/cholesterol-enriched domains (lipid rafts) and the ld phase to the rest of the membrane, rich in the low T_m lipid (in both cases, DOPC).

Fig. 4 shows AFM images recorded in the liquid cell of a DOPC/DPPC/cholesterol SLB deposited on mica, in the absence of ethanol, and after successive additions of ethanol. In the pristine bilayer (panel

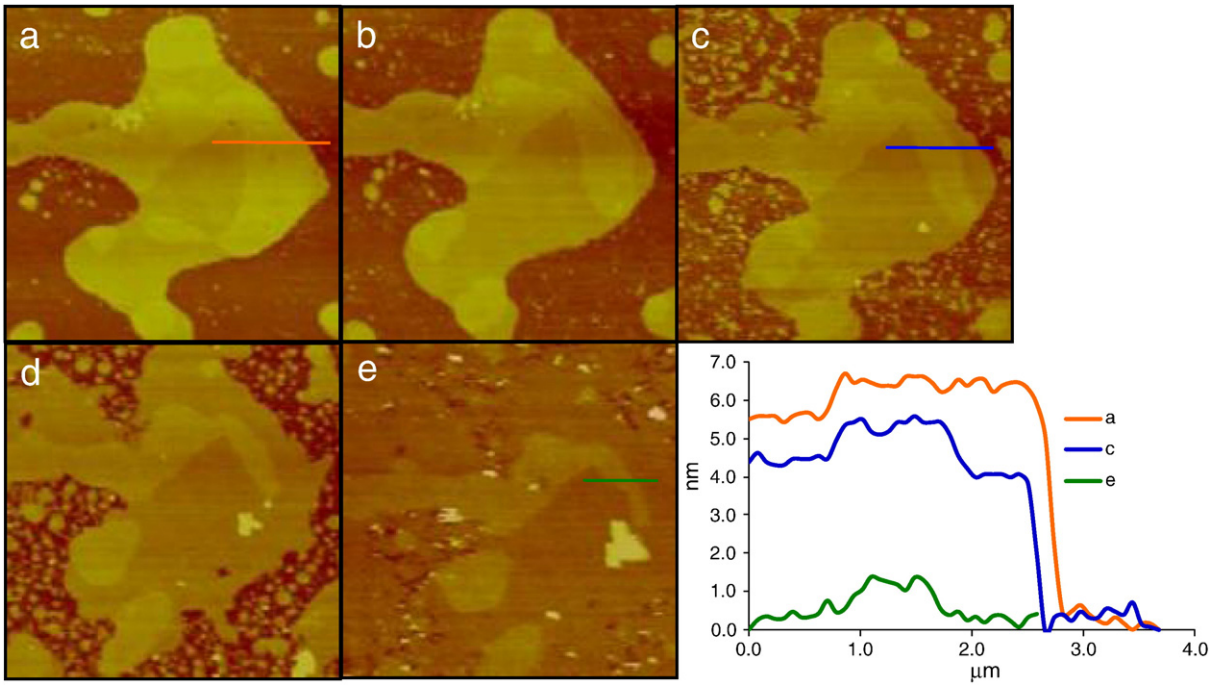

Fig. 4. Ethanol interactions with a bilayer displaying ld/lo phase separation (lipid rafts) on mica. AFM image of an SLB composed of DOPC/DPPC/cholesterol (40:40:20 mol:mol:mol) deposited on mica, a) in the absence of ethanol, and after successive additions of ethanol to a final concentration of b) 8%; c) 13%; d) 20%; and f) 25% (v/v) in Hepes buffer. The images were obtained in a liquid cell at room temperature. The inset shows the topographical profiles corresponding to the colored lines in panels a–e. The images correspond to an area of 11 μm × 11 μm. $Z = 15$ nm.

a), the coexistence of ld and lo domains with a height difference of 1.2 nm is clearly observed (Table 1). For this lipid system the area fraction of lo domains (Table 2) is similar to the one predicted by the phase diagram [56]. Upon addition of ethanol to a concentration of 8% (v/v) (Fig. 4b), the topography of the system remained essentially unchanged. However, when the concentration of ethanol reached 13% (v/v) (Fig. 4c), both ld and lo domains became thinner by ~1.1 nm, as demonstrated by the topographical profiles of Fig. 4 and Table 1. The whole bilayer has undergone thickness reduction simultaneously, to a similar height value as the fluid phase in DOPC/DPPC mixtures for high ethanol concentration (22%). This behavior is completely distinct from the one observed for the gel/fluid coexistence (Figs. 1 and 2), and shows how the membrane composition and lateral organization strongly influence ethanol-induced alterations. With successive additions of ethanol other effects become apparent: with 20% (v/v) ethanol (Fig. 4d), the area fraction occupied by thinner (more disordered) domains becomes larger; for higher concentrations of ethanol (Fig. 4e), pronounced bilayer expansion is observed.

Fig. 5 shows the results of a similar study where the high T_m lipid is PSM instead of DPPC. Through the comparison of the results obtained for this system with those described in the previous paragraph, it will be possible to understand if the type of ordered domains present in the membrane is the ruling factor determining ethanol-induced effects, or if these are highly dependent on the particular high T_m lipid. Again, the clear coexistence of ld and lo domains is observed in Fig. 5a, and the ld/lo area fractions (Table 2) are in good accordance with the phase diagram [62]. The height difference between the domains is 1.0 nm (see also inset with topographical profile in Fig. 5 and Table 1), in agreement with a previous study of an analogous system [63]. Upon addition of ethanol to a final concentration of 4% (v/v) (Fig. 5b), no significant changes were detected. However, at 13% (v/v) of ethanol (Fig. 5c) the whole bilayer undergoes a reduction of its thickness around 1.2 nm for ld domains and 1.0 nm for lo domains. Thus, the system DOPC/PSM/cholesterol behaves in a similar manner as the DOPC/DPPC/cholesterol. Further additions of ethanol cause an increase of the area fraction occupied by ld domains since only this portion of the bilayer expands significantly as a result of the interaction with ethanol (Fig. 5d, Table 2).

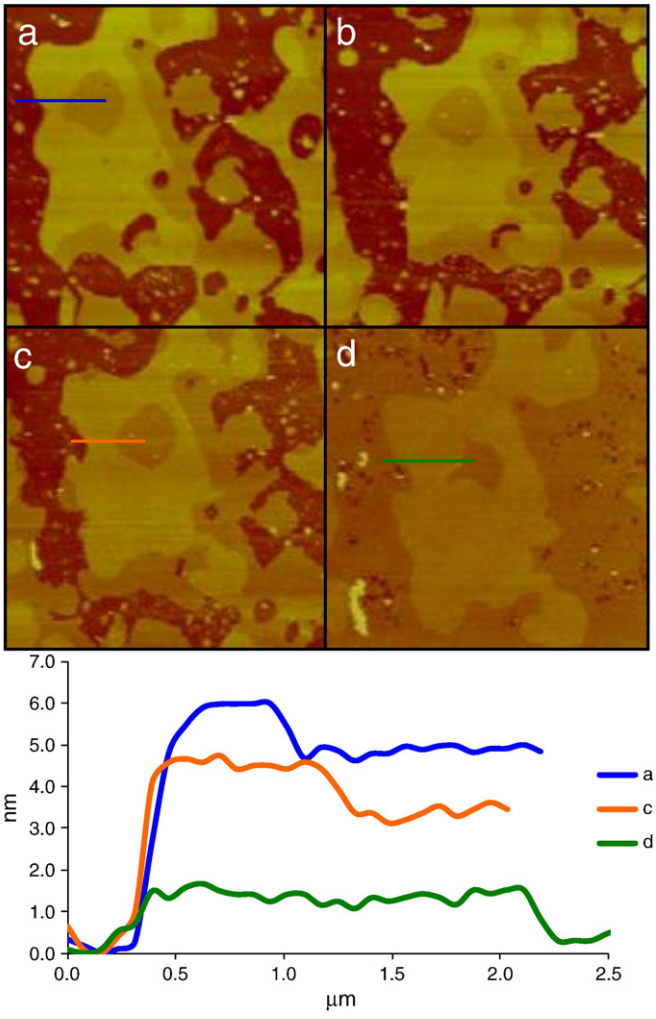

Fig. 5. Ethanol interactions with a bilayer containing sphingomyelin and with ld/lo phase separation (lipid rafts) on mica. AFM image of an SLB composed of DOPC/PSM/cholesterol (40:40:20 mol:mol:mol) deposited on mica, (a) in the absence of ethanol, and after successive additions of ethanol to a final concentration of (b) 4%, (c) 13%, and (d) 25% (v/v) in Hepes buffer. The images were obtained in a liquid cell at room temperature. The inset shows the topographical profiles corresponding to the colored lines in panels a–d. The images correspond to an area of 11 μm × 11 μm. $Z = 15$ nm.

3.4. Lipid bilayers deposited on silicon

The influence of ethanol on DPPC bilayers was studied using silicon as substrate (Fig. 6). As mentioned in the Introduction, ethanol–DPPC interactions were thoroughly addressed in the literature using mica as a substrate, but not silicon. In the absence of ethanol the DPPC bilayer thickness on silicon (~6.2 nm; panel a) is close to the one observed for mica surfaces (Supplementary Fig. S2a) and for low ethanol concentrations, no significant alterations were observed. At 20% (v/v) ethanol concentration (Fig. 6b) some portions of the bilayer become thinner and the difference between thin domains and unmodified bilayer is similar to the one obtained on mica (Table 1). Furthermore, for high ethanol concentrations (30%, v/v) bilayer expansion with almost complete coverage of the observation area also happened (Fig. 6c). The final height reduction observed in pure DPPC is close to 2 nm, as reported by several authors for DPPC bilayers on mica [12,64]. This height reduction is similar to the one observed for DPPC-enriched gel domains in DOPC/DPPC bilayers. However, in the binary gel domains, a significant expansion of the gel as detected in pure DPPC bilayers was not observed, pointing to a role for gel/fluid coexistence in the outcome of ethanol effects.

The effect of ethanol in PSM-containing lipid rafts was also performed for bilayers deposited on silicon (Fig. 7). With this substrate, ld/lo phase separation was also observed for the DOPC/PSM/cholesterol (40:40:20) mixture (Fig. 7a). However, the area fraction of ordered phase is smaller than for SLB of the same composition deposited in mica (Table 2). Recently, a similar behavior was observed with DOPC/1,2-distearoyl-sn-glycero-3-phosphocholine (DSPC)/cholesterol bilayers supported in silica xerogel where the fraction of the ordered domains was lower than the one expected from the phase diagram and observed on mica. The authors attributed this difference to curvature-induced mechanisms [65]. The average size and shape of the domains is also influenced by the substrate, since it can be clearly seen that they are different when a bilayer of the same composition is formed on mica (Fig. 5). In Fig. 7 it is shown that upon successive ethanol additions to DOPC/PSM/cholesterol SLB on silicon, the following effects were observed: simultaneous thickness reduction for both ld and lo domains (panels b and c) of 1.3 nm, and bilayer expansion of ld domains with respective increased fractional area of these domains (panels c and d), i.e., qualitatively the same behavior as noticed in mica (Fig. 5). The extent of expansion (Table 2) was comparable to the one observed in mica for intermediate ethanol concentrations (13%). It was not possible to obtain good quality images of SLB in silicon for higher ethanol concentrations.

4. Discussion

In this work, the interaction of ethanol with lipid bilayers presenting different lipid number and/or types of lipid phases was

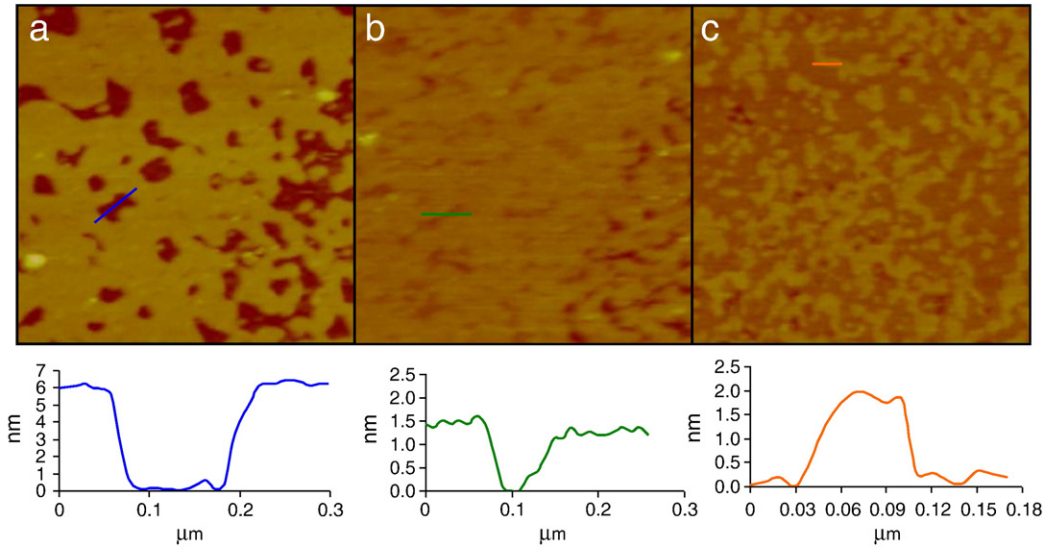

Fig. 6. Ethanol interactions with a bilayer in the gel phase deposited on silicon. AFM image of an SLB composed of DPPC deposited on silicon, after successive additions of ethanol to a final concentration of (a) 0%, (b) 20%, and (c) 30% (v/v) in PBS buffer. The images were obtained in a liquid cell at room temperature. The insets show the topographical profiles corresponding to the colored lines in panels a–c. The images correspond to an area of 1.5 µm × 1.5 µm. $Z = 20$ nm.

studied by AFM. The main goal of this work was to determine to what extent the presence and type of lipid domains, namely gel/fluid domains, and ld/lo domains (lipid rafts) modulate the ethanol-induced membrane changes. In addition, it was also intended to determine the consequences of progressively increase ethanol concentration in the hydration medium of the lipids.

In general, the observations here reported can be correlated with previously published studies [20–22] of ethanol–bilayer interactions, using single-phase lipid bilayers, either free-standing or on solid supports, mica and silicon. This was confirmed by studying the role of small amounts of cholesterol in the promotion of interdigitation of gel phase bilayers shown in the present work on mica SLBs (Fig. 3), and previously reported for silicon SLBs studied by ellipsometry [51]. Moreover, the phase mole fractions obtained in mica in phase separating mixtures are coincident with the published phase diagrams for free-standing bilayers [56,62].

On silicon, bilayer thickness reduction was observed for gel phase SLB (DPPC, Fig. 6), and for ternary fluid bilayers of DOPC/PSM/cholesterol (Fig. 7), being this latter a better model for the lipid composition of the outer leaflet of mammalian plasma membrane. Similar effects were observed for this ternary mixture deposited on mica. Although the solid support has an influence on bilayer organization, possibly due to surface effects such as frictional coupling [66], the substrate used is not determining the outcome of ethanol–bilayer interactions, except for high ethanol concentrations, because in this case the ternary lipid bilayer becomes unstable when supported on silicon. However, the substrate may influence the amounts of ethanol necessary for observing the same effect as in free-standing bilayers [38], as discussed below, and also the ld/lo phase fractions and domain morphology, since on silicon they are different from those on mica [65] and giant vesicles [62].

DPPC is one of the few cases where ethanol-induced interdigitation has been unequivocally observed from the analysis of the electron density profiles obtained by X-ray diffraction [21]. The height and area alterations reported there are in agreement with the results obtained in the present AFM study for both ethanol–DPPC on silicon, and for the gel phase DPPC/cholesterol (98:2) on mica (Tables 1 and 2). The height difference between tilted liquid expanded and upright liquid condensed DPPC monolayers or bilayers is ~0.6 nm [32], indicating that the ~2 nm height reduction induced by ethanol on gel phase SLBs (Table 1) is not explained solely by tilting.

In the present study, even for high ethanol concentrations, the gel phase SLB is not fully interdigitated, which is not in agreement with the established phase diagrams [21,33,38]. However, it should be pointed out that in the present study ethanol was added sequentially to pre-formed SLBs, requiring the use of higher ethanol concentrations in order to observe similar effects. This has been previously described, and recently it was shown that incubating the vesicles with ethanol above the phospholipid T_m is necessary for quantitative agreement between SLBs and free-standing bilayers [38,51]. Note that in most studies with free-standing bilayers, the lipid is hydrated with ethanol/water mixtures and subjected to heating/cooling cycles. To this respect, the results of the present work are in agreement with the typical SLB behavior.

The study of the mixture DOPC/DPPC revealed the presence of gel domains coexisting with fluid domains, separated by a height difference of ~1.2 nm (Table 1), as previously described [34,60]. When interacting with this mixture ethanol induces a first bilayer thickness reduction, that is larger for the fluid domains, and only at higher concentrations the second thickness reduction is larger for the gel domains (Fig. 1). The membrane partitioning of ethanol is less propitious into saturated/ordered bilayers than into unsaturated/disordered ones [67]. Moreover, the increase of fluid phase fraction relatively to gel fraction was observed as a consequence of the fluid phase expansion in response to ethanol interaction while gel domains maintain their total area (Table 2). The area calculated considering volume conservation is very similar to the one experimentally observed. If the reduction in gel phase fraction is also taken into consideration in the estimated areas, then volume conservation is verified. In this case it is possible to quantitatively compare the results with those obtained by micropipette aspiration in SOPC fluid bilayers in the presence of ethanol [68,69]. The authors observed a thickness reduction and area increase up to 10–15% due to water/bilayer interfacial tension reduction, which leads to an expansion of the lipid bilayer because the lipid headgroups are less tightly packed [68], possibly becoming more disordered and/or more tilted. However, the first height reduction observed for the fluid in the present work was much higher (~1.3 nm), hence an additional mechanism should be accountable. DOPC has a very low T_m and therefore at room temperature the degree of disorder is already quite large. In addition, for very disordered acyl chains it is difficult to infer on tilting, due to their high mobility and lack of organization. It is possible that,

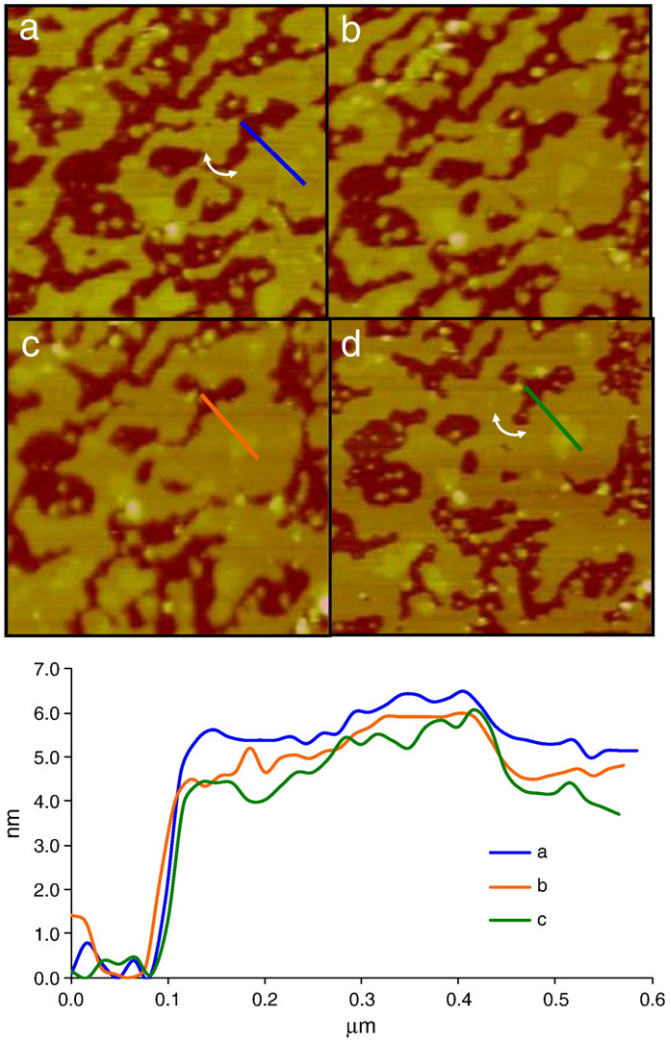

Fig. 7. Ethanol interactions with a bilayer containing sphingomyelin displaying ld/lo phase separation (lipid rafts) on silicon. AFM image of an SLB composed of DOPC/PSM/cholesterol (40:40:20 mol:mol:mol) deposited on silicon, before (a) and after successive additions of ethanol to a final concentration of (b) 4%, (c) 8%, and (d) 13% (v/v) in Hepes buffer. The images were obtained in a liquid cell at room temperature. The inset shows the topographical profiles corresponding to the colored lines in panels a–d. The images correspond to an area of 2.0 μm × 2.0 μm. $Z = 15$ nm. The curved white arrows highlight bilayer expansion as seen by increased substrate coverage.

together with disordering or tilting, a partial interpenetration of the acyl chains from one leaflet to the other is occurring, which is different from the interdigitation reported for gel phase in pure DPPC. The formation of partially interdigitated phases does not affect significantly the lateral mobility of the phospholipids [70], which is compatible with a fluid phase, particularly with highly disordered unsaturated chains [71]. A similar mechanism has been proposed for pure DOPC bilayer expansion and thinning induced by an increase of the temperature from 40 to 50 °C as determined by AFM in liquid [72]. Recent molecular dynamics simulations predicted the formation of interdigitated structures in fluid bilayers in the presence of moderately high ethanol concentrations [73]. Regarding the gel domains, due to its significant fraction decrease, it is not possible to offer a unique molecular description of the process. However, it should be noted that the thickness reduction (1.8 nm) is similar to the one observed for pure DPPC reported in the literature [12,64] and in the present work for DPPC on silicon (1.8 nm) and DPPC/cholesterol 98:2 in mica (1.9 nm) (Figs. 6 and 3, respectively). In the gel phase the phospholipid acyl chains are arranged in a hexagonal packing as a consequence of *trans*-configuration of the phospholipid acyl chains which results in the almost complete absence of free volume inside of the bilayer [74,75]. The effects of ethanol on DPPC-enriched gel may thus be explained by interdigitation, concomitantly with a large decrease of gel phase fraction, thereby maintaining the gel phase area. However, this interdigitation occurs only for very high ethanol concentrations due to the preferential interaction of ethanol with the fluid, and thus it should have limited biological significance. The tilting that is probably responsible for the first 0.4 nm thinning of the gel domains is much more plausible to occur in very ordered domains in biological systems.

Finally, one more worth noting observation in the DOPC/DPPC mixture is that the region where the first thickness reduction domains start to form depends on the domain organization. Thinner fluid domains appear inside gel domains when these are discontinuous and the fluid phase is prominent (Fig. 2), whereas they appear at the gel-fluid interface surrounding fluid domains when these are discontinuous and minor (Fig. 1). There is both theoretical [61] and experimental [18,76,77] evidence that the dynamic wetting layer effects at gel/fluid interfaces become less influential when the gel phase fraction is increased, particularly when it becomes the continuous phase, and that the interfacial lipid is maximal near phase coexistence boundaries. Accordingly, ethanol would act more easily inside the gel domains at the corrugation defects in the 1:1 mixture, whereas the less rigid and more prevalent gel/fluid interfaces would be the preferential targets for ethanol in the gel-enriched mixture. The observed increase of fluid domains fraction (Table 2) is related to the fact that ethanol interacts preferentially with this phase, enhancing its stability relatively to the gel phase. While this can be partially explained by a freezing point depression (see e.g. [30]), the more complex effects relating the sites of first thickness reduction to which domains are discontinuous cannot be fully accounted by this single thermodynamic consideration.

The use of lipid raft-forming ternary mixtures provided additional evidence for the importance of membrane domain organization on the interaction with ethanol. In the case of ld/lo phase separation, in two different systems (DOPC/DPPC/cholesterol and DOPC/PSM/cholesterol), thickness reduction occurred for a relatively low ethanol concentration and to a similar extent for both ordered and disordered domains (Figs. 4 and 5), a behavior distinct from the one observed for the gel/fluid DOPC/DPPC mixture. This is a reflex of the fluid nature of both phases present in the ternary mixtures. To better understand ethanol effects on those mixtures, area and volume calculations were also performed (Table 2). Similarly to what was detected for DOPC/DPPC, it is clear that the disordered phase has undergone expansion, while ordered domains, in this case lo phase, did not experience significant area variations (Table 2). Thus, a clear increase of the disordered fraction occurred. Since there was no detectable change in the area of the ordered domains, despite the height reduction of this fraction, plausibly due to disordering/tilting of the acyl chains and partial interdigitation, as described for DOPC-enriched fluid phase in DOPC/DPPC bilayers, it is implied that part of the lipids of lo domains were transferred to the ld phase. With 13% ethanol, the changes in the disordered phase are comparable to those described above in the case of gel/fluid coexistence. However, for higher ethanol concentration, a much larger expansion took place, which cannot be solely explained by means of disordering, tilting or partial interpenetration. The degree of expansion observed could be justified by the opening of the acyl chains of each phospholipid, similarly to the reported extended lipid conformation [78,79] or through their looping, as described for other lipids [80]. In the case of DOPC/PSM/cholesterol, the interaction between ethanol and the lipid bilayer follows the trends discussed above, except that the estimated final expansion (Table 2) was smaller. However, a total coverage of the substrate was reached for both ternary mixtures, in contrast to the observed for the binary gel/fluid system. The second height reduction of the fluid phase in DOPC/

DPPC is only of 0.3 nm. However, this takes place when significant fluid phase expansion occurs in that system. Thus, an opening of the acyl chains may be occurring, but more limited than in the ternary lipid mixtures, possibly due to the presence of cholesterol.

Ethanol affects bilayer thickness and also the domain organization of the membrane, thus its biological effects can be exerted by affecting the functions associated with membrane proteins whose location and activity are dependent on bilayer thickness and also on domain structure [81–83].

Finally, bilayer expansion was always observed for high ethanol concentrations, suggesting that this can be a useful strategy for an improved lipid coating of solid substrates that can be used either to better study membrane related phenomena, or to design technological devices based on lipid–water interfaces [84,85]. To this respect the observation of bilayer expansion leading to increased surface coverage in silicon is particularly relevant.

5. Conclusions

The present work demonstrates the ability of AFM to unravel details from the nano to the micro scale of the interaction between ethanol and complex lipid systems. The study of binary and ternary lipid systems has shown that this alcohol interacts preferentially with the most disordered phase, promoting an increase of its fraction. The thickness reduction of the fluid phase with increasing ethanol concentrations in the absence of cholesterol can be explained by an interfacial tension reduction for low ethanol concentrations, accompanied by additional disordering/tilting and/or partial interdigitation (~1.3 nm) and then by a slight aperture of the acyl chains (0.3 nm and more pronounced expansion). In the lipid rafts-mimicking ternary mixtures, these effects play a role also for lower ethanol concentrations (~1 nm thickness reduction) and for higher alcohol levels a dramatic bilayer expansion, possibly involving acyl chain extended conformations or looping, occurs. It was also shown that ethanol effects were similar on both ternary lipid systems studied (lo/ld coexistence), whereas gel/fluid and lo/ld bilayers present a different behavior in response to ethanol. As a consequence ethanol action should be more dependent on the type of domains present than on the type of lipid.

Finally, qualitatively similar ethanol effects were observed for bilayers deposited on mica and silicon, demonstrating that the major effects are not dependent on the substrate used for the formation of SLB. However, the domain organization is clearly different and ethanol effects are not completely comparable at a quantitative level.

Supplementary materials related to this article can be found online at doi:10.1016/j.bbamem.2010.10.006.

Acknowledgements

A.S.V. and R.F.M.D. acknowledge funding from F.C.T., Portugal, received through the Centre of Chemistry and Biochemistry and research grant PTDC/QUI/66612/2006. J.T.M. acknowledges PhD scholarship SFRH/BD/64442/2009.

References

[1] R.F.M. de Almeida, L.M.S. Loura, M. Prieto, Membrane lipid domains and rafts: current applications of fluorescence lifetime spectroscopy and imaging, Chem. Phys. Lipids 157 (2009) 61–77.
[2] A. Kusumi, C. Nakada, K. Ritchie, K. Murase, K. Suzuki, H. Murakoshi, R.S. Kasai, J. Kondo, T. Fujiwara, Paradigm shift of the plasma membrane concept from the two-dimensional continuum fluid to the partitioned fluid: high-speed single-molecule tracking of membrane molecules, Annu. Rev. Biophys. Biomol. Struct. 34 (2005) 351-U54.
[3] R.G.W. Anderson, K. Jacobson, Cell biology—a role for lipid shells in targeting proteins to caveolae, rafts, and other lipid domains, Science 296 (2002) 1821–1825.
[4] R.F.M. de Almeida, A. Fedorov, M. Prieto, Sphingomyelin/phosphatidylcholine/cholesterol phase diagram: boundaries and composition of lipid rafts, Biophys. J. 85 (2003) 2406–2416.
[5] M. Stockl, A.P. Plazzo, T. Korte, A. Herrmann, Detection of lipid domains in model and cell membranes by fluorescence lifetime imaging microscopy of fluorescent lipid analogues, J. Biol. Chem. 283 (2008) 30828–30837.
[6] C.D. Blanchette, W.C. Lin, C.A. Orme, T.V. Ratto, M.L. Longo, Domain nucleation rates and interfacial line tensions in supported bilayers of ternary mixtures containing galactosylceramide, Biophys. J. 94 (2008) 2691–2697.
[7] P.E. Milhiet, C. Domec, M.C. Giocondi, N. Van Mau, F. Heitz, C. Le Grimellec, Domain formation in models of the renal brush border membrane outer leaflet, Biophys. J. 81 (2001) 547–555.
[8] R.F.M. de Almeida, L.M.S. Loura, A. Fedorov, M. Prieto, Lipid rafts have different sizes depending on membrane composition: a time-resolved fluorescence resonance energy transfer study, J. Mol. Biol. 346 (2005) 1109–1120.
[9] M.C. Giocondi, P.E. Milhiet, P. Dosset, C. Le Grimellec, Use of cyclodextrin for AFM monitoring of model raft formation, Biophys. J. 86 (2004) 861–869.
[10] A. Bunge, P. Muller, M. Stockl, A. Herrmann, D. Huster, Characterization of the ternary mixture of sphingomyelin, POPC, and cholesterol: support for an inhomogeneous lipid distribution at high temperatures, Biophys. J. 94 (2008) 2680–2690.
[11] L.C. Silva, R.F.M. de Almeida, B.M. Castro, A. Fedorov, M. Prieto, Ceramide-domain formation and collapse in lipid rafts: membrane reorganization by an apoptotic lipid, Biophys. J. 92 (2007) 502–516.
[12] Z.V. Leonenko, D.T. Cramb, Revisiting lipid - general anesthetic interactions (I): thinned domain formation in supported planar bilayers induced by halothane and ethanol, Can. J. Chem. Rev. Can. Chim. 82 (2004) 1128–1138.
[13] L.G. Shamrakov, D.T. Cramb, Induced structural changes of a supported planar bilayer after exposure to halothane—a real-time atomic force microscopy study, Can. J. Chem. Rev. Can. Chim. 83 (2005) 1190–1194.
[14] Z. Leonenko, E. Finot, D. Cramb, AFM study of interaction forces in supported planar DPPC bilayers in the presence of general anesthetic halothane, Biochim. Biophys. Acta (BBA)-Biomembr. 1758 (2006) 487–492.
[15] F. Schroeder, T. Hubbell, S.M. Colles, W.G. Wood, Expression of liver fatty-acid-binding protein in L-cells - plasma-membrane response to ethanol, Arch. Biochem. Biophys. 316 (1995) 343–352.
[16] D.M. Lovinger, Alcohols and neurotransmitter gated ion channels: past, present and future, Naunyn-Schmiedebergs Arch. Pharmacol. 356 (1997) 267–282.
[17] F. Schroeder, S.M. Colles, G.P. Kreishman, C.E. Heyliger, W.G. Wood, Synaptic Plasma-membrane structure and polarity of long-sleep and short-sleep mice, Arch. Biochem. Biophys. 309 (1994) 369–376.
[18] R.F.M. de Almeida, L.M.S. Loura, A. Fedorov, M. Prieto, Nonequilibrium phenomena in the phase separation of a two-component lipid bilayer, Biophys. J. 82 (2002) 823–834.
[19] G.P. Casey, W.M.M. Ingledew, Ethanol tolerance in yeasts, CRC Crit. Rev. Microbiol. 13 (1986) 219–280.
[20] S.A. Simon, T.J. Mcintosh, Interdigitated hydrocarbon chain packing causes the biphasic transition behavior in lipid alcohol suspensions, Biochim. Biophys. Acta 773 (1984) 169–172.
[21] U. Vierl, L. Lobbecke, N. Nagel, G. Cevc, Solute effects on the colloidal and phase behavior of lipid bilayer membranes: ethanol–dipalmitoylphosphatidylcholine mixtures, Biophys. J. 67 (1994) 1067–1079.
[22] M.F.N. Rosser, H.M. Lu, P. Dea, Effects of alcohols on lipid bilayers with and without cholesterol: the dipalmitoylphosphatidylcholine system, Biophys. Chem. 81 (1999) 33–44.
[23] T.J. Mcintosh, H.N. Lin, S.S. Li, C.H. Huang, The effect of ethanol on the phase transition temperature and the phase structure of monounsaturated phosphatidylcholines, Biochim. Biophys. Acta-Biomembr. 1510 (2001) 219–230.
[24] H. Komatsu, E.S. Rowe, Effect of cholesterol on the ethanol-induced interdigitated gel phase in phosphatidylcholine—use of fluorophore pyrene-labeled phosphatidylcholine, Biochemistry 30 (1991) 2463–2470.
[25] F. Schroeder, W.J. Morrison, C. Gorka, W.G. Wood, Transbilayer effects of ethanol on fluidity of brain membrane leaflets, Biochim. Biophys. Acta 946 (1988) 85–94.
[26] H.E. Schueler, R.J. Hitzemann, R.A. Harris, G.P. Kreishman, Ethanol-induced differential disordering of the surface of synaptic plasma membranes from mice selected for genetic differences in ethanol intoxication, Prog. Clin. Biol. Res. 292 (1989) 425–434.
[27] J.A. Barry, K. Gawrisch, Direct Nmr evidence for ethanol binding to the lipid–water interface of phospholipid-bilayers, Biochemistry 33 (1994) 8082–8088.
[28] L.L. Holte, K. Gawrisch, Determining ethanol distribution in phospholipid multilayers with MAS-NOESY spectra, Biochemistry 36 (1997) 4669–4674.
[29] J.H. Chin, D.B. Goldstein, Drug tolerance in biomembranes—spin label study of effects of ethanol, Science 196 (1977) 684–685.
[30] T. Heimburg, A.D. Jackson, The thermodynamics of general anesthesia, Biophys. J. 92 (2007) 3159–3165.
[31] J.A. Barry, K. Gawrisch, Effects of ethanol on lipid bilayers containing cholesterol, gangliosides, and sphingomyelin, Biochemistry 34 (1995) 8852–8860.
[32] C.W. Hollars, R.C. Dunn, Submicron structure in L-alpha-dipalmitoylphosphatidylcholine monolayers and bilayers probed with confocal, atomic force, and near-field microscopy, Biophys. J. 75 (1998) 342–353.
[33] K.J. Tierney, D.E. Block, M.L. Longo, Elasticity and phase behavior of DPPC membrane modulated by cholesterol, ergosterol, and ethanol, Biophys. J. 89 (2005) 2481–2493.
[34] A. Berquand, M.P. Mingeot-Leclercq, Y.F. Dufrene, Real-time imaging of drug-membrane interactions by atomic force microscopy, Biochim. Biophys. Acta-Biomembr. 1664 (2004) 198–205.

[35] E.S. Rowe, Induction of lateral phase separations in binary lipid mixtures by alcohol, Biochemistry 26 (1987) 46–51.
[36] C. Trandum, P. Westh, K. Jorgensen, O.G. Mouritsen, Association of ethanol with lipid membranes containing cholesterol, sphingomyelin and ganglioside: a titration calorimetry study, Biochim. Biophys. Acta-Biomembr. 1420 (1999) 179–188.
[37] C. Trandum, P. Westh, K. Jorgensen, O.G. Mouritsen, A thermodynamic study of the effects of cholesterol on the interaction between liposomes and ethanol, Biophys. J. 78 (2000) 2486–2492.
[38] J.M. Vanegas, R. Faller, M.L. Longo, Influence of ethanol on lipid/sterol membranes: phase diagram construction from AFM imaging, Langmuir 26 (2010) 10415–10418.
[39] L.J. Pike, Lipid rafts: heterogeneity on the high seas, Biochem. J. 378 (2004) 281–292.
[40] P. Sengupta, B. Baird, D. Holowka, Lipid rafts, fluid/fluid phase separation, and their relevance to plasma membrane structure and function, Semin. Cell Dev. Biol. 18 (2007) 583–590.
[41] D.A. Brown, E. London, Functions of lipid rafts in biological membranes, Annu. Rev. Cell Dev. Biol. 14 (1998) 111–136.
[42] M.P. Mingeot-Leclercq, M. Deleu, R. Brasseur, Y.F. Dufrene, Atomic force microscopy of supported lipid bilayers, Nat. Protoc. 3 (2008) 1654–1659.
[43] M.C. Giocondi, D. Yamamoto, E. Lesniewska, P.E. Milhiet, T. Ando, C. Le Grimellec, Surface topography of membrane domains, Biochim. Biophys. Acta (BBA)-Biomembr. 1798 (2010) 703–718.
[44] C. Leidy, T. Kaasgaard, J.H. Crowe, O.G. Mouritsen, K. Jorgensen, Ripples and the formation of anisotropic lipid domains: imaging two-component supported double bilayers by atomic force microscopy, Biophys. J. 83 (2002) 2625–2633.
[45] M.C. Howland, A.W. Szmodis, B. Sanii, A.N. Parikh, Characterization of physical properties of supported phospholipid membranes using imaging ellipsometry at optical wavelengths, Biophys. J. 92 (2007) 1306–1317.
[46] M. Sundh, S. Svedhem, D.S. Sutherland, Influence of phase separating lipids on supported lipid bilayer formation at SiO2 surfaces, Phys. Chem. Chem. Phys. 12 (2010) 453–460.
[47] I. Pfeiffer, B. Seantier, S. Petronis, D. Sutherland, B. Kasemo, M. Zach, Influence of nanotopography on phospholipid bilayer formation on silicon dioxide, J. Phys. Chem. B 112 (2008) 5175–5181.
[48] A.P. Quist, A. Chand, S. Ramachandran, C. Daraio, S. Jin, R. Lal, Atomic force microscopy imaging and electrical recording of lipid bilayers supported over microfabricated silicon chip nanopores: lab-on-a-chip system for lipid membranes and ion channels, Langmuir 23 (2007) 1375–1380.
[49] R. Zeineldin, J.A. Last, A.L. Slade, L.K. Ista, P. Bisong, M.J. O'Brien, S.R.J. Brueck, D.Y. Sasaki, G.P. Lopez, Using bicellar mixtures to form supported and suspended lipid bilayers on silicon chips, Langmuir 22 (2006) 8163–8168.
[50] A. Miszta, B. van Deursen, R. Schoufs, M. Hof, W.T. Hermens, Absence of ethanol-induced interdigitation in supported phospholipid bilayers on silica surfaces, Langmuir 24 (2008) 19–21.
[51] M. Gedig, S. Faiss, A. Janshoff, Melting and interdigitation of microstructured solid supported membranes quantified by imaging ellipsometry, Biointerphases 3 (2008) FA51–FA58.
[52] C.W.F. Mcclare, Accurate and convenient organic phosphorus assay, Analytical Biochemistry 39 (1971) 527–530.
[53] M. Benes, D. Billy, A. Benda, H. Speijer, M. Hof, W.T. Hermens, Surface-dependent transitions during self-assembly of phospholipid membranes on mica, silica, and glass, Langmuir 20 (2004) 10129–10137.
[54] I. Reviakine, A. Brisson, Formation of supported phospholipid bilayers from unilamellar vesicles investigated by atomic force microscopy, Langmuir 16 (2000) 1806–1815.
[55] R.L. McClain, J.J. Breen, The image-based observation of the L beta I-to-L-beta ' phase transition in solid-supported lipid bilayers, Langmuir 17 (2001) 5121–5124.
[56] R.F.M. de Almeida, J. Borst, A. Fedorov, M. Prieto, A.J.W.G. Visser, Complexity of lipid domains and rafts in giant unilamellar vesicles revealed by combining imaging and microscopic and macroscopic time-resolved fluorescence, Biophys. J. 93 (2007) 539–553.
[57] B.R. Lentz, Y. Barenholz, T.E. Thompson, Fluorescence depolarization studies of phase-transitions and fluidity in phospholipid bilayers. 2. Two-component phosphatidylcholine liposomes, Biochemistry 15 (1976) 4529–4537.
[58] E.S. Rowe, Lipid chain-length and temperature-dependence of ethanol phosphatidylcholine interactions, Biochemistry 22 (1983) 3299–3305.
[59] D. Marsh, Thermodynamic analysis of chain-melting transition temperatures for monounsaturated phospholipid membranes: dependence on cis-monoenoic double bond position, Biophys. J. 77 (1999) 953–963.
[60] S. Morandat, K. El Kirat, Solubilization of supported lipid membranes by octyl glucoside observed by time-lapse atomic force microscopy, Colloids Surf., B 55 (2007) 179–184.
[61] K. Jorgensen, O.G. Mouritsen, Phase separation dynamics and lateral organization of two-component lipid membranes, Biophys. J. 69 (1995) 942–954.
[62] S.L. Veatch, S.L. Keller, Miscibility phase diagrams of giant vesicles containing sphingomyelin, Phys. Rev. Lett. 94 (2005).
[63] C.B. Yuan, J. Furlong, P. Burgos, L.J. Johnston, The size of lipid rafts: an atomic force microscopy study of ganglioside GM1 domains in sphingomyelin/DOPC/cholesterol membranes, Biophys. J. 82 (2002) 2526–2535.
[64] J.X. Mou, J. Yang, C. Huang, Z.F. Shao, Alcohol induces interdigitated domains in unilamellar phosphatidylcholine bilayers, Biochemistry 33 (1994) 9981–9985.
[65] E.I. Goksu, M.L. Longo, Ternary lipid bilayers containing cholesterol in a high curvature silica xerogel environment, Langmuir 26 (11) (2010) 8614–8624. doi: 10.1021/la9046885.
[66] Y. Kaizuka, J.T. Groves, Structure and dynamics of supported intermembrane junctions, Biophys. J. 86 (2004) 905–912.
[67] E. Terama, O.H.S. Ollila, E. Salonen, A.C. Rowat, C. Trandum, P. Westh, M. Patra, M. Karttunen, I. Vattulainen, Influence of ethanol on lipid membranes: from lateral pressure profiles to dynamics and partitioning, J. Phys. Chem. B 112 (2008) 4131–4139.
[68] H.V. Ly, M.L. Longo, The influence of short-chain alcohols on interfacial tension, mechanical properties, area/molecule, and permeability of fluid lipid bilayers, Biophys. J. 87 (2004) 1013–1033.
[69] H.V. Ly, D.E. Block, M.L. Longo, Interfacial tension effect of ethanol on lipid bilayer rigidity, stability, and area/molecule: a micropipet aspiration approach, Langmuir 18 (2002) 8988–8995.
[70] V. Schram, T.E. Thompson, Interdigitation does not affect translational diffusion of lipids in liquid crystalline bilayers, Biophys. J. 69 (1995) 2517–2520.
[71] M. Mihailescu, K. Gawrisch, The structure of polyunsaturated lipid bilayers important for rhodopsin function: a neutron diffraction study, Biophys. J. 90 (2006) L04–L06.
[72] Z.V. Leonenko, E. Finot, H. Ma, T.E.S. Dahms, D.T. Cramb, Investigation of temperature-induced phase transitions in DOPC and DPPC phospholipid bilayers using temperature-controlled scanning force microscopy, Biophys. J. 86 (2004) 3783–3793.
[73] A.N. Dickey, R. Faller, How alcohol chain-length and concentration modulate hydrogen bond formation in a lipid bilayer, Biophys. J. 92 (2007) 2366–2376.
[74] P.F.F. Almeida, W.L.C. Vaz, T.E. Thompson, Lateral diffusion in the liquid-phases of dimyristoylphosphatidylcholine cholesterol lipid bilayers—a free-volume analysis, Biochemistry 31 (1992) 6739–6747.
[75] P.F.F. Almeida, W.L.C. Vaz, T.E. Thompson, Lipid diffusion, free area, and molecular dynamics simulations, Biophys. J. 88 (2005) 4434–4438.
[76] G. Leidy, W.F. Wolkers, K. Jorgensen, O.G. Mouritsen, J.H. Crowe, Lateral organization and domain formation in a two-component lipid membrane system, Biophys. J. 80 (2001) 1819–1828.
[77] K. Jorgensen, A. Klinger, R.L. Biltonen, Nonequilibrium lipid domain growth in the gel-fluid two-phase region of a DC16PC-DC22PC lipid mixture investigated by Monte Carlo computer simulation, FT-IR, and fluorescence spectroscopy, J. Phys. Chem. B 104 (2000) 11763–11773.
[78] J.P. Mattila, K. Sabatini, P.K.J. Kinnunen, Interaction of cytochrome c with 1-palmitoyl-2-azelaoyl-sn-glycero-3-phosphocholine: evidence for acyl chain reversal, Langmuir 24 (2008) 4157–4160.
[79] E. Kalanxhi, C.J.A. Wallace, Cytochrome c impaled: investigation of the extended lipid anchorage of a soluble protein to mitochondrial membrane models, Biochem. J. 407 (2007) 179–187.
[80] A. Chattopadhyay, E. London, Parallax method for direct measurement of membrane penetration depth utilizing fluorescence quenching by spin-labeled phospholipids, Biochemistry 26 (1987) 39–45.
[81] T.K.M. Nyholm, S. Ozdirekcan, J.A. Killian, How protein transmembrane segments sense the lipid environment, Biochemistry 46 (2007) 1457–1465.
[82] M.C. Giocondi, F. Besson, P. Dosset, P.E. Milhiet, C. Le Grimellec, Remodeling of ordered membrane domains by GPI-Anchored intestinal alkaline phosphatase, Langmuir 23 (2007) 9358–9364.
[83] E. Sparr, W.L. Ash, P.V. Nazarov, D.T.S. Rijkers, M.A. Hemminga, D.P. Tieleman, J.A. Killian, Self-association of transmembrane alpha-helices in model membranes - Importance of helix orientation and role of hydrophobic mismatch, J. Biol. Chem. 280 (2005) 39324–39331.
[84] M.I. Fisher, T. Tjarnhage, Structure and activity of lipid membrane biosensor surfaces studied with atomic force microscopy and a resonant mirror, Biosens. Bioelectron. 15 (2000) 463–471.
[85] E. Reimhult, K. Kumar, Membrane biosensor platforms using nano- and microporous supports, Trends Biotechnol. 26 (2008) 82–89.